LAWRENCE
LIVERMORE
NATIONAL
LABORATORY

# Centroid Stabilization in Alignment of FOA Corner Cube:Designing of a Match Filter

A. Awwal, K. Wilhelmsen, R. Roberts, R. Leach, R. Lowe-Webb, T. Ngo

January 27, 2015

**Disclaimer**

This document was prepared as an account of work sponsored by an agency of the United States government. Neither the United States government nor Lawrence Livermore National Security, LLC, nor any of their employees makes any warranty, expressed or implied, or assumes any legal liability or responsibility for the accuracy, completeness, or usefulness of any information, apparatus, product, or process disclosed, or represents that its use would not infringe privately owned rights. Reference herein to any specific commercial product, process, or service by trade name, trademark, manufacturer, or otherwise does not necessarily constitute or imply its endorsement, recommendation, or favoring by the United States government or Lawrence Livermore National Security, LLC. The views and opinions of authors expressed herein do not necessarily state or reflect those of the United States government or Lawrence Livermore National Security, LLC, and shall not be used for advertising or product endorsement purposes.

# Centroid stabilization in alignment of FOA Corner Cube: designing of a match filter

Abdul Awwal, Karl Wilhelmsen, Randy Roberts, Richard Leach, Roger Lowe-Webb and Tony Ngo
Lawrence Livermore National Laboratory, Livermore, CA. 94551
E-mail: awwal1@llnl.gov

## ABSTRACT

The current automation of image-based alignment of NIF high energy laser beams is providing the capability of executing multiple target shots per day. An important aspect of performing multiple shots in a day is to reduce additional time spent aligning specific beams due to perturbations in those beam images. One such alignment is that of the final optics assembly (FOA). The FOA is the optical element that aligns the beams into the final target chamber. Beam-to-beam variations and systematic beam changes over time in the FOA can lead to a reduction in accuracy as well as increased convergence durations for the template based centroid detector. This work presents a systematic approach of maintaining FOA corner cube centroid templates so that stable position estimation is applied thereby leading to fast convergence of alignment control loops. In the matched filtering approach, a template is designed based on most recent images taken in the last 60 days. The results show that new filter reduces the divergence of the position estimation of FOA images.

Keywords: laser alignment, position detection, template matching, matched filter, image processing and analysis, correlation peak, beam alignment, High power laser.

## 1. INTRODUCTION

The National Ignition Facility (NIF) is a megajoule-class solid-state laser and targeting facility constructed by the Department of Energy at the Lawrence Livermore National Laboratory (LLNL). NIF was built with three main goals: 1) to examine new regimes of astrophysics as well as basic science, 2) to ensure the U.S. stockpile of nuclear weapons remain safe, secure and 3) reliable and to create fusion ignition and energy gain in a laboratory setting which will lead to an almost limitless supply of safe, carbon-free, electricity [1].
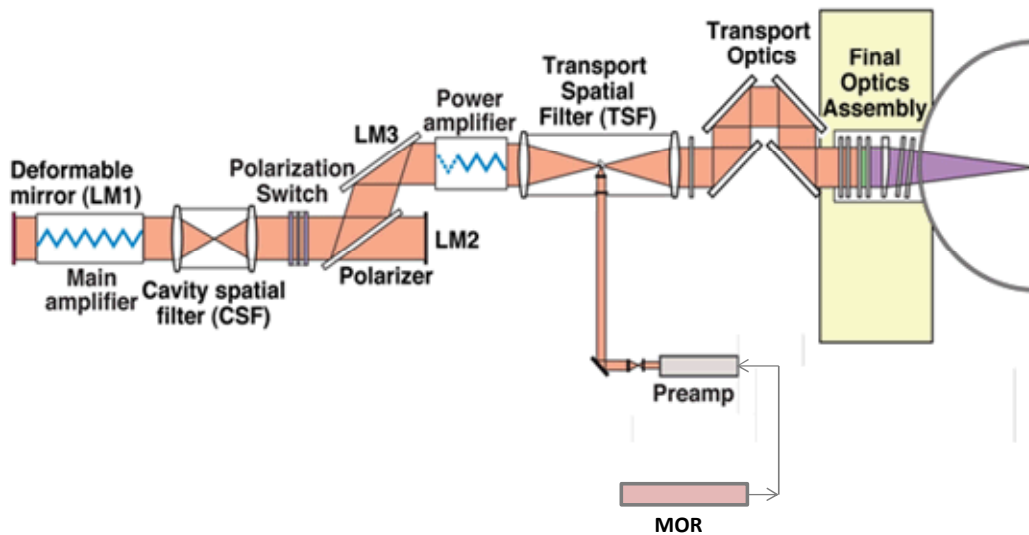


Figure 1. A beam path from start to finish

Figure 1 traces a complete path of a single beamline for the NIF laser. A laser pulse at wavelength 1053 nm originating from the master oscillator (MOR) is split and amplified by 48 preamplifiers that contain two different amplification stages that increase the pulse's energy by a factor of 10 billion. The 48 beams are then split into four beams each for injection into the 192 main laser amplifier beamlines. Each beam is then amplified by two systems of large glass amplifiers, first the power amplifier and then the main amplifier. In the main amplifier, a Pockels cell switch forces the light to bounce back and forth four times, while deformable mirrors compensate the wavefront to ensure the beams are uniform, smooth and have high wavefront quality. From the main amplifier, the beam makes another pass through the power amplifier. At this time, the beams' total energy has grown from 1 billionth of a joule to 1.8 million joules. The 192 amplified beams are guided by two ten-story switchyards on either side of the target chamber to the 10m diameter target chamber. NIF's laser beams travel about 1,500 meters from their origin to their destination at the center of the spherical target chamber. From start to finish these beams are aligned using an Automated Alignment system that takes 30 minutes to complete [2-4].

NIF's 192 beams are arranged into quads and fed into the target chamber. At the entrance to the target chamber, final optics assemblies (FOAs) frequency convert each beam to the third harmonic of 351 nm and focus them onto the target. Each FOA consists of a fixed system interface to the target chamber, and four integrated optics modules (IOMs). These precision opto-mechanical systems perform frequency conversion, color separation, beam sampling, vacuum isolation, and debris shielding [5].

The FOA optical configuration is shown schematically in Figure 2. A fused silica lens focuses the frequency converted 3ω light onto the target. The lens and the frequency conversion crystals are precision mounted in a cell to provide the required alignment precision. Precision alignment is carried out by inserting a corner cube into the FOA. The corner cube is a retro reflector that positions the laser beam at the target as the laser travels through a vacuum window. The corner cubes are placed on a carriage rail and moved into the beam before the 1ω phase plate for alignment. A critical image processing task in FOA alignment is to estimate the centroid position of two beam spot patterns that appear in the corner cube images captured by a CCD camera. Determining high precision spot centroid locations in the FOA corner cube images has been a long-standing challenge in the NIF Final Optics Assembly [6].
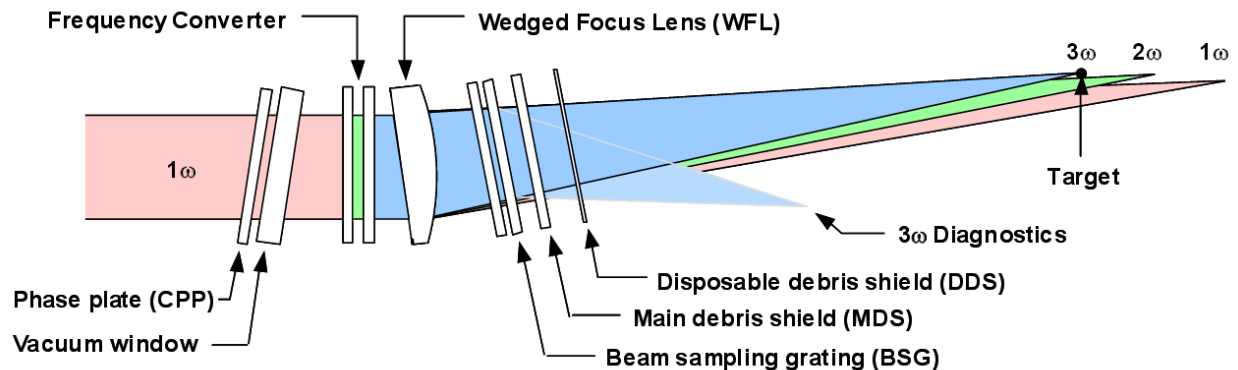


Figure 2. Final optics assembly (FOA) schematic configuration

The initial step in performing main laser beam alignment is to establish a reference position at beam center. Next a sequence of measurements is made using an alignment laser source. The laser fires creating a test beam that propagates through a sequence of mirrors through the spatial filter to the FOA. Here two corner cube[1] reflectors reflect the beam back to a CCD camera where the "FOA alignment image" is produced. The image in Figure 3 consists (ideally) of two horizontally spaced circles; the position estimate is taken as the bisector of a line segment through the centers. The function of the FOA algorithm is to find the centroids of the two FOA corner cube images within 0.5 pixels.

In this paper, we describe a method of detecting the center of the corner cube images using a matched filter. The optimization process to choose the filter from a number of possible designs is elucidated. The objective of the design is

---

[1] A corner cube reflector is a cube that is cut to have three mutually perpendicular faces with the property that it is retrodirective, that is, it reflects all incoming rays back along their original directions.

to reduce the variance of position estimation when there is no mechanical movement. After describing the background information in the next section, we list various methods used in this paper for developing a suitable template, and then in the following section we explain the numerical optimization process.
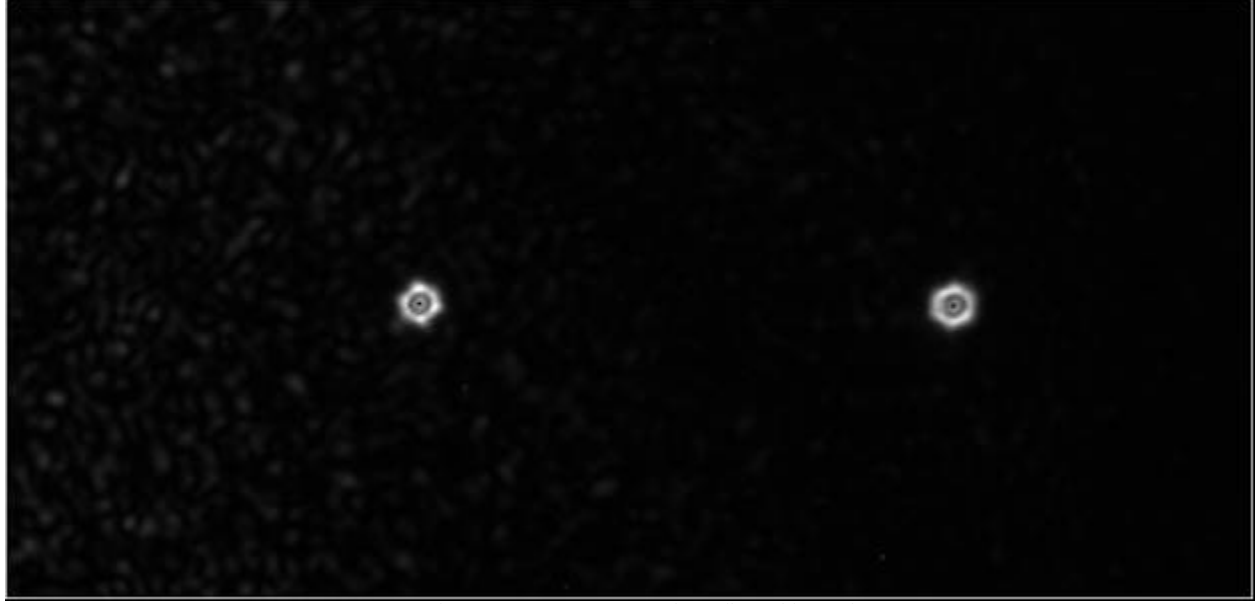


Figure 3. FOA corner cube reflected beam image

## 2. BACKGROUND

The complex matched filter (CMF) is well known for its position detection capability where the position of the object can be derived from the position of the correlation peak. A CMF [7] can be defined by assuming that the Fourier transform of the object function $f$(x,y) is denoted by:

$$F(U_x, U_y) = |F(U_x, U_y)| \exp(j\Phi(U_x, U_y)) \tag{1}$$

The CMF for detecting the function $f$(x,y) and its location, is given by the complex conjugate of the Fourier spectrum $F(U_x, U_y)$ as denoted in Eq. 2,

$$H_{CMF}(U_x, U_y) = F^*(U_x, U_y) = |F(U_x, U_y)| \exp(-j\Phi(U_x, U_y)) \tag{2}$$

The shape of correlation and the discrimination capability of CMF are usually not as good as that of a phase only filter or amplitude modulated correlation filter (AMPOF) [8,9]. A modified phase only filter (POF) was designed based on the following formulation:

$$H_{POF}(U_x, U_y) = H_{CMF} / (\alpha + |F(U_x, U_y)|) \tag{3}$$

Where the parameter α is used to ensure minimum variance in position estimation. When we have a class of objects that needs to be detected with slight variation of internal structure, intensity, gradient and noise, a composite filter may be exploited to capture all these variations into a single template [10]. The position of the object can be found from the position of the cross correlation, autocorrelation, and the template using Eqs. 4(a-b).

$$X_{pos} = X_{cross} - X_{auto} + X_c \qquad\qquad \textbf{(4a)}$$

$$y_{pos} = y_{cross} - y_{auto} + y_c \qquad\qquad \textbf{(4b)}$$

The value of $(x_{pos}, y_{pos})$ is the to-be-determined position of the pattern in the image plane. The value of $(x_{auto}, y_{auto})$ is the position of the template autocorrelation peaks and the value of $(x_{cross}, y_{cross})$ is the position of the cross correlation peak. The position of the cross-correlation peak is estimated using a polynomial fit of second order to the correlation peak. The center of the template, $(x_c, y_c)$ is calculated offline, using a centroiding method and verified visually. The $(x_{auto}, y_{auto})$ are calculated off-line. An illustration of the equation 4(a-b) is depicted in Fig. 4. A pulse shown on the top left of Fig. 4, is assumed to be the template, centered on $x_c = 15$. By default the origin is assumed to be at 0. When an autocorrelation is performed, the resulting correlation function will be a triangular pulse centered on 0. In an optical or 2-D digital image processing, the origin of the output plane is usually centered on the middle of the plane. Shifting the origin to a hypothetical middle-of-plane point 300, we get $x_{auto} = 300$. Now consider wanting to detect a pulse located at 605. The cross-correlation of the input with the to-be-detected pulse will be centered on 890 at the shifted origin of 300. It is a simple exercise to verify that the pulse position (605) can be obtained easily from the values of the cross, auto and template position. This same technique is applied in detecting a 2-D object except the same calculation is extended to a 2-D image plane.
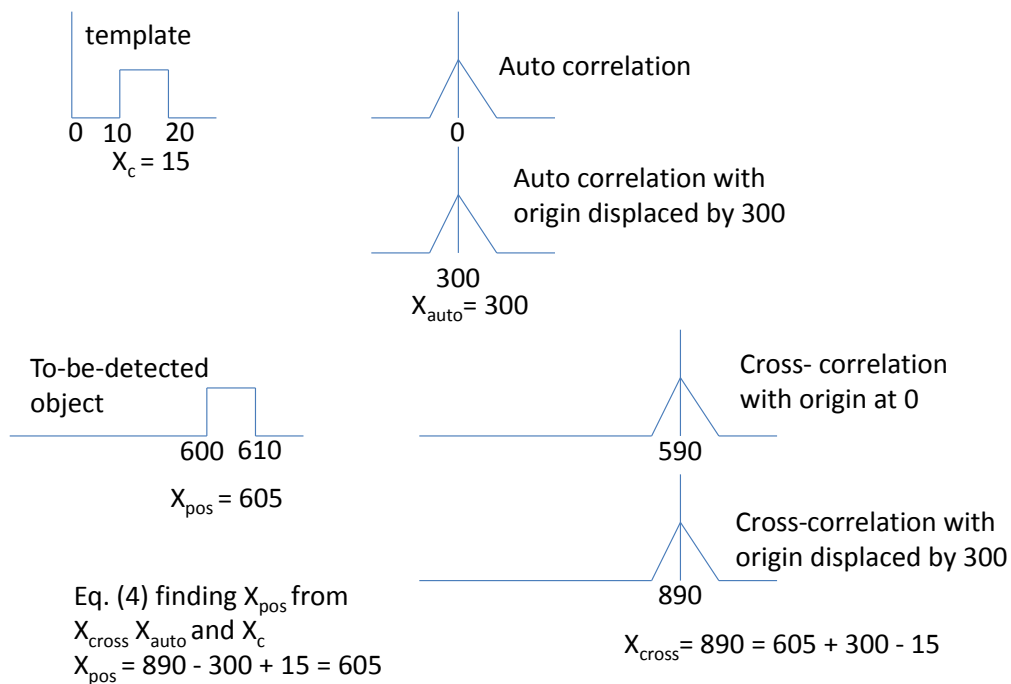


Figure 4: Relationship of positions of correlation peak with those of the template and the assumed origin location in 1-D.

The correlation is performed in the Fourier domain by multiplying the complex conjugate of the Fourier transformed template with the transform of the input image. The peak is detected by interpolating a second order polynomial near the correlation peak. The displacement of the cross-correlation is used to find the location of the object.

## 3. TEMPLATE FORMULATION

The FOA corner cube reflected beam image is shown in Fig. 3. The left FOA spot is tilted to the left and right one tilted to the right. The brightness of the right spot shows a thick brighter region to the left of its center position. The robustness and stability of the position of the detected patterns depends on appropriate selection of an optimum template. If the position is not stable, then the position will change with the instantaneous intensity and the alignment loop will be unstable or take a long time to converge. The different types of templates considered for position detection are described below:

**Ideal template:** This template is constructed from one of the 192 beamlines which clearly shows the diagonal line features of the corner cube image as shown in Fig. 5(b). Under ideal imaging condition, all 192 FOAs should look like the ideal one. The advantage of this approach is that all the beams will have the same template therefore the maintenance of the templates become easier. However, for practical reasons of varying imaging and illumination condition, the beam images as shown in Fig. 3, differ greatly from the ideal image.

**Separate left and right template**: The above may not work in all cases, where the left and right spots are very different. In that case, left and right templates are required to be separated. This is accomplished using a single image, as the previous case, or an average of multiple images. Thus, to detect the position of the left spot, a left template is designed from average of many images. Likewise, the right averaged spot can be taken as template for determining the right spot. Using two templates for two objects makes the correlation process more involved, since now two separate matching operations have to be performed instead of a single one.

**Composite template:** To overcome the problem of having two separate templates, a composite template may be designed which provides a strong match for both left and right spots. A composite may be generated from a single image as above or from average recent historic images. For optimal performance, the left and right templates are combined with a certain weight as shown in Fig. 5(a).
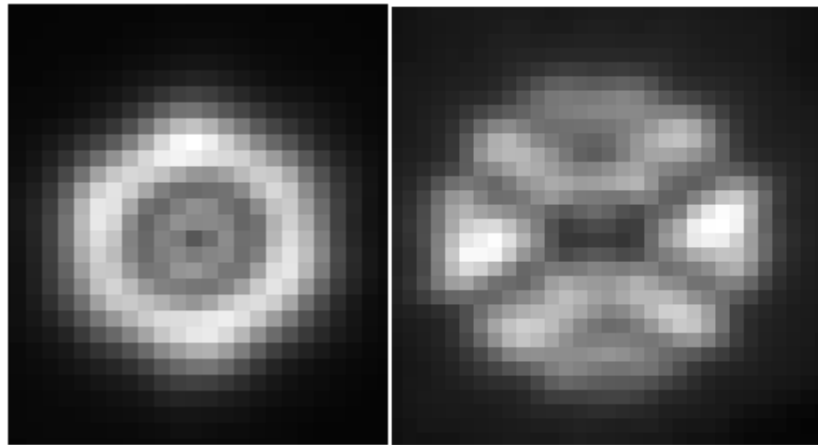


Figure 5. (a) Composite template formed by averaging left, right images from 133 real images from last six months (June 2014 – Nov 2014) (b) An ideal template used from a well-focused FOA beam line.

**Averaging**: Averaging could also be used in all the above cases, whether composite or multiple templates are desired. Three different processes of averaging were used in the construction of composite templates. For each beamline, an initial reference template is constructed, using a single image. Using this initial template, the positions of the rest of the set are determined and registered with respect to each other to a common center location. An average image is then

constructed from the registered set. For registration several techniques were considered. In one case, an integer amount of movement was performed. In the second case, the images were expanded 5 times and then translated in the expanded domain. This resulted in movements of as low as 0.2 pixels. The images were then scaled back to the original size. In the third case, the images were kept in the original space but a rounded displacement was performed for registration.

After choosing a specific filter from the above categories, the CMF (Eq. 2) and POF (Eq. 3) with various values of α were considered. A typical correlation plane output is depicted in Fig. 6. The figure shows the presence of intense speckle noise towards the left spot due to nonuniform illumination. The position is then calculated from Eq. 4. When multiple image data set from same beamline are evaluated, a typical scatter plot is obtained as depicted in Fig. 7. When each of the above filters is formed, 8 variations are tested.
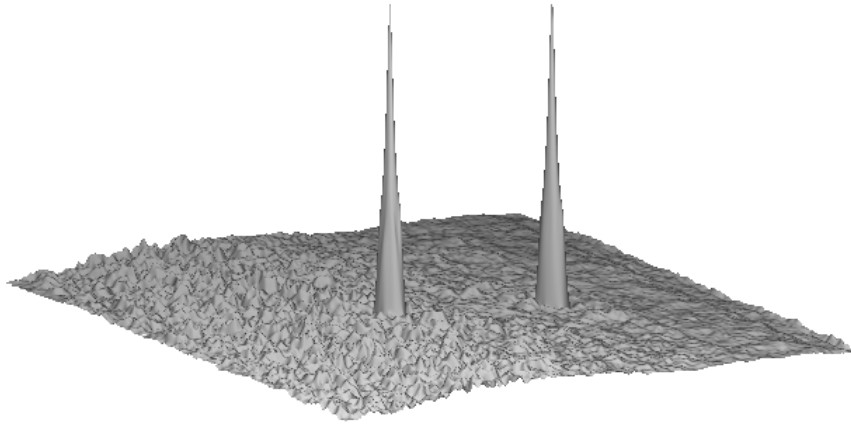
Figure 6. The correlation plane output for a composite template
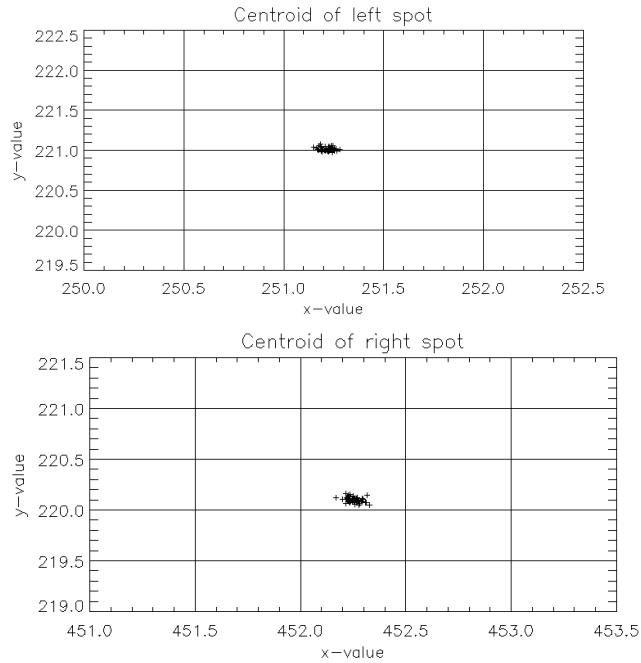
Figure 7. Scatter plot of left and right fiducial of FOA corner cube image

# 4. DESIGN AND SELECTION OF BEST FILTER

The various prescriptions of templates described in Section 3 were constructed and a set of experiments were performed. The dataset used for the experiment consisted of a set of 50 FOA images taken from the same beamline consecutively without moving any mechanical parts. These 50 images are ideally at the same position, since, no devices were moved; however, they have sufficient feature variations so that each position may be slightly different. Thus the left and right position data should have minimal divergence, as well as the distance between the spots. For each of the above templates several key parameters were observed. These parameters are calculated from position data as shown in Fig. 7 and tabulated in Fig. 8. In addition, CMF and POF with various values of α were evaluated. Typical outputs of the parameters are

```
POF used...
POF used alpha =  0.00100000
Radial Three Sigma-for left_x,y    0.115252
Radial Three Sigma-right,x_y    0.121813
Standard deviation of distances    0.0414177
Mean left, x,y    251.219    221.014
Mean right, x,y    452.254    220.101
Range of left-x    0.134689
Range of left-y    0.106354
Range of right-x    0.161346
Range of right-y    0.110764
Range of d    0.187332
Mean distance    201.037
Total error =    1.06180
```

Filter: B415_composite_tmplt_round2.tif

Figure 8. Parameters for performance

Total error = sum of all the above errors, the standard deviation of distances were multiplied by 3 to get the 3 sigma number. The first parameter α is used in Eq. 3. The radial three sigma deviations are for the left and right spot position data, a typical set shown in Fig. 7. As can be seen from Fig. 7 and also the Table 8 that the three sigma values are bounded by .15 pixels whereas the range of all the spots in Fig. 7 are less than 0.2 pixels. The mean value of each distribution is listed in Table 8 and can be seen in Fig. 7. The distance between the spots is the radial distance between the left and right centroid and are plotted for the 50 images in Fig. 9. The standard deviation of the distance is also another figure of merit and added into the total error calculation after multiplying by three. All the other errors are of the same scale.
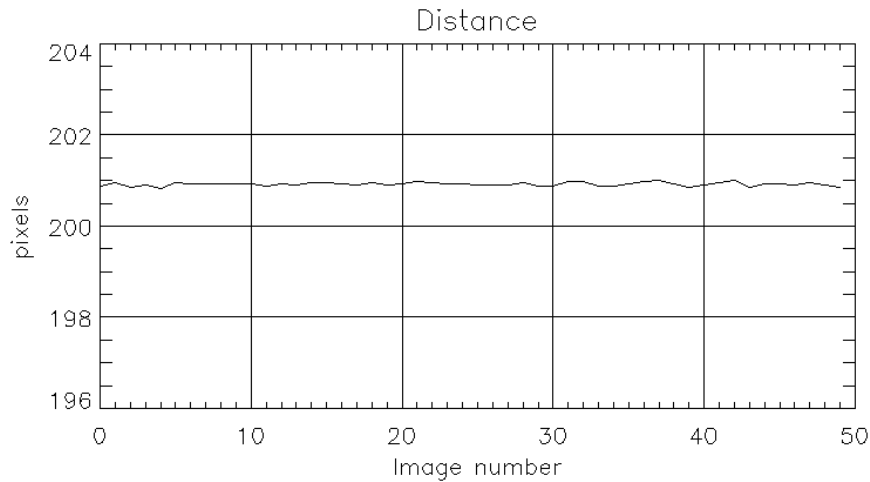


Figure 9. Distance between spots for 50 images

**Testing Ideal template**: When an ideal template as shown in Fig. 5(b) was tested with the 50 image data set, results were not very satisfactory and not repeatable. A typical output is shown in Fig. 10.
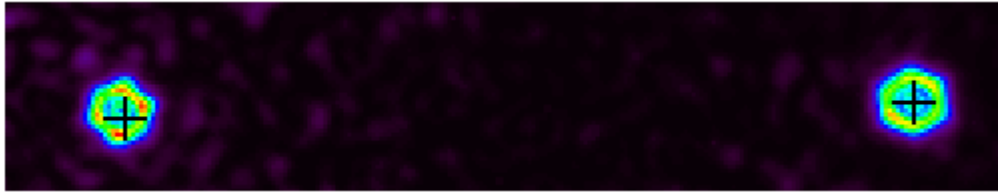


Figure 10. Location from an ideal template, for an image from 50 image dataset.

As can be seen from Fig. 10, the position on the left spot is not well centered. When testing the ideal template on a different beamline as shown in Fig. 11, the position was found to vary by almost 5 pixels in terms of relative position on the beam as shown below. This is clearly not a good choice of template for our specific beam in consideration. Next we constructed the template from the beam image itself.
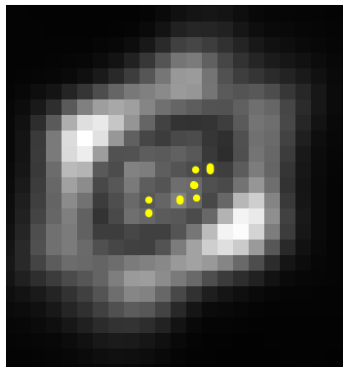


Figure 11. Relative locations from an ideal template, mapping of locations for a typical beam.

**Testing Left/right template**: The idea here is to use a separate template for both patterns from the current beamline. One hundred and thirty three historic images were averaged using integer shift registration and averaging technique. Then both left and right patterns from this average were applied. It was found the left pattern resulted in a 0.137 3-sigma radius for the left spot and right average template resulted 3-sigma radius of 0.126 pixels.

**Evaluating Composite template**: The composite template was constructed from the average of one hundred and thirty three images [11] from the same beamline. Thereafter the left and right spot patterns were averaged. A template made from a single beam was used to align the left and right side before averaging. Multiple options were considered in the averaging of the left and right templates in terms of intensity normalization, displacement rounding, and what to add to the mixture of the composite template. In some cases, the left and right images were normalized before adding, in other cases, they were not normalized. Experimentally, combining two left and right templates without normalization produced the overall best result. Also we experimented with adding or not adding the template used to align the left and right patterns. Adding a single beam template produced the better result. Once the first generation composite template was made, it was used in aligning the second generation of template. This was carried out by replacing single beam template with the composite and is expected to further fine tune the registration.

The set of all experiments with a certain template is shown in Fig. 12. The first entry is the CMF, thereafter 7 variations of POF were considered with a value of $\alpha = 0,0.0001,0.001,0.005,0.01,0.025$, and $0.05$. For this particular implementation of composite filter the best value is for AMPOF with $\alpha = 0.05$ with minimum error 1.13597. However, with all the implementation of the filters, the filter output shown in Fig. 8, with $\alpha = 0.001$ shows the best minimal error with error of 1.06180. In this particular filter, image registration was performed by rounding the displacement of various images before averaging. After averaging, the image was multiplied by a circular mask to eliminate the noise outside the template pattern. The right template was added in with the composite with an equal weight as the left and right averages.

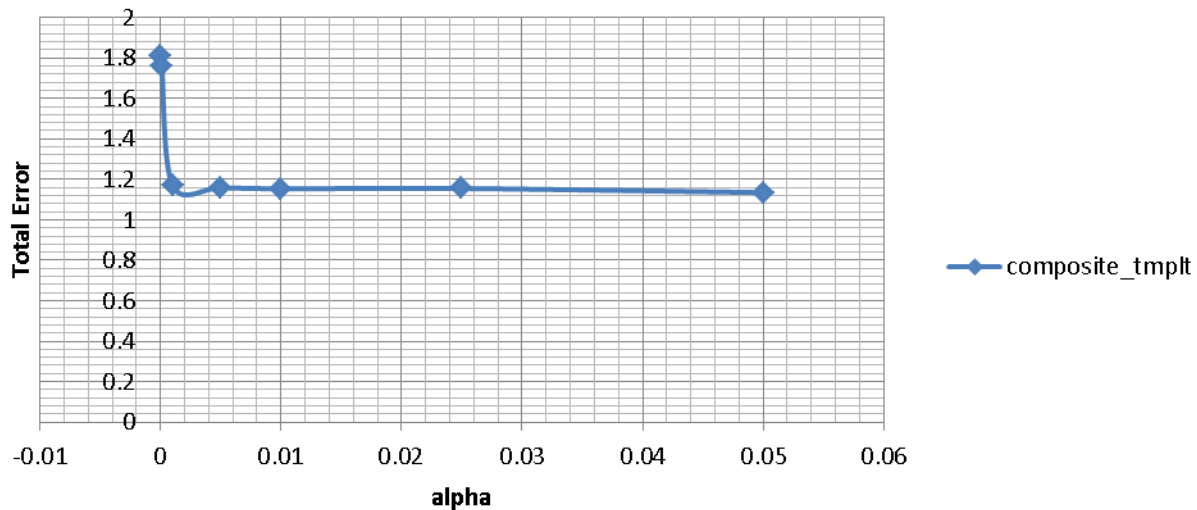## Optimization of composite filter



Figure 12. Optimization results from one specific filter.

## 5. CONCLUSIONS

In this work, a method of developing an optimum composite filter for FOA corner cubes is illustrated. The method compares various formulations of composite filters and selects the optimum one in terms of minimum total error. Many formulations of combining the images to form a composite were evaluated. Only the most significant results are reported. The method described here is simple, repeatable and can be performed for all 192 beams.

## ACKNOWLEDGEMENT

## REFERENCES

[1] J. Lindl, and Moses, E. "Plans for the National Ignition campaign (NIC) on the National Ignition Facility (NIF): On the threshold of initiating ignition experiments," Special issue of Physics of Plasmas 5, 050901-1, (2011)

[2] S. C. Burkhart, E. Bliss, D. Kalantar, R. Lowe-Webb, T. McCarville, D. Nelson, … K. Wilhelmsen, "National Ignition Facility system alignment," *Applied Optics, 50*(8), 1136-57 (2011).

[3] K. Wilhelmsen, A. Awwal, W. Ferguson, B Horowitz, V. Miller Kamm, C. Reynolds, "Automatic Alignment System For The National Ignition Facility," Proceedings of 2007 International Conference on Accelerator and Large Experimental Control Systems (ICALEPCS07), 486-490 (2007).

[4] J. V. Candy, W. A. McClay, A. A. S. Awwal, and S. W. Ferguson, "Optimal position estimation for the automatic alignment of a high-energy laser," Journal of Optical Society of America A, Vol. 22, pp. 1348-1356 (2005).

[5] Paul J. Wegner ; Jerome M. Auerbach ; Thomas A. Biesiada, Jr. ; Sham N. Dixit ; Janice K. Lawson ; Joseph A. Menapace ; Thomas G. Parham ; David W. Swift ; Pamela K. Whitman and Wade H. Williams, "NIF final optics system: frequency conversion and beam conditioning", Proc. SPIE 5341, Optical Engineering at the Lawrence Livermore National Laboratory II: The National Ignition Facility, 180 (2004).

[6] Wilbert A. McClay III, Abdul A. S. Awwal, Scott C. Burkhart, James V. Candy, "Optimization and improvement of FOA corner cube algorithm", in Photonic Devices and Algorithms for Computing VI, Khan M. Iftekharuddin; Abdul Ahad S. Awwal, Editors, Proceedings of SPIE Vol. 5556 (SPIE, Bellingham, WA 2004), pp.227-232.

[7]  M. A. Karim and A. A. S. Awwal, Optical Computing: An Introduction, John Wiley, New York, NY (1992).

[8]  A. A. S. Awwal, M. A. Karim, and S. R. Jahan, "Improved Correlation Discrimination Using an Amplitude-modulated Phase-Only Filter," *Applied Optics*, Vol. 29, pp. 233-236, 1990.

[9]  A. A. S. Awwal, "What can we learn from the shape of a correlation peak for position estimation?," Applied Optics, Vol. 49, pp. B41-B50, (2010).

[10] M. Rahman, A. A. S. Awwal, and K. Gudmundsson,  "Composite Filters for Search Time Reduction for 3D Model Based Object Recognition," *Photonic Devices and Algorithms for Computing V*, K.M. Iftekharuddin and A. A. S. Awwal Editors, Proc. of SPIE, Vol. 4201, 2003.

[11] A. A. S. Awwal, Wilbert A. McClay, Walter S. Ferguson, James V. Candy, Thad Salmon, and Paul Wegner, "Detection and Tracking of the Back-Reflection of KDP Images in the presence or absence of a Phase mask," Applied Optics, Vol. 45, pp. 3038-3048, May 2006.